L.O. Copy Mr. R.S. Templin

L.O.	NATIONAL AERONAUTICAL ESTABLISHMENT OTTAWA, CANADA	NO. AE-81b HSAL-M-83
FILE BM2-17-13A-12	LABORATORY MEMORANDUM	PAGE 1 OF
PREPARED BY J.L. and J.A. vdB.		COPY NO 4
CHECKED BY JL	SECTION Aerodynamics	DATE 17 May 1957.

SECURITY CLASSIFICATION ~~Confidential~~

SUBJECT Directional Stability Tests at M=1.57 on a 1/80 Scale Model of the Avro C-105 Aircraft with Certain Modifications.

PREPARED BY J. Lukasiewicz
J. A. van der Bliek

ISSUED TO Dr. D. C. MacPhail
Mr. J. H. Parkin
Mr. R. J. Templin (2)
Mr. J. Lukasiewicz (2)
Mr. J. A. van der Bliek
Aero Library (2)

Summary

Factors affecting directional stability are reviewed in relation to the C-105 configuration.

Flow visualization and force tests were carried out at M=1.57 on standard C-105 configuration and on 5 modifications involving ventral fins, wing fins, enlarged vertical tail and wing fences. The results of tests indicated in general favourable effects of four modifications on directional stability.

Comparison with NACA data indicates satisfactory agreement.

Contents

List of Symbols

b = wing span, in.

c = local chord length, in.

$\bar{c}$ = mean aerodynamic chord, in.

c_o = root chord length, in.

$C_l = \frac{l}{qSb}$ = rolling moment coefficient

$C_{l_\beta} = \partial C_l / \partial \beta$ = rolling moment derivative, per deg.

$C_n = \frac{n}{qSb}$ = yawing moment coefficient

$C_{n_\beta} = \partial C_n / \partial \beta$ = yawing moment derivative, per deg.

$C_Y = \frac{Y}{qSb}$ = side force coefficient

$C_{Y_{loc}}$ = local side force coefficient

$C_{Y_\beta} = \partial C_Y / \partial \beta$ = side force derivative, per deg.

l = rolling moment, in.lb.

M = Mach number

n = yawing moment, in.lb.

q = dynamic pressure, p.s.i.

S = gross wing area, sq. in.

v_σ = side wash velocity

Y = side force, lb.

α = angle of attack, deg.

β = angle of yaw, deg.

ΔS = increment in side area due to modification, sq. in.

ΔC_{n_β}, ΔC_{l_β}, ΔC_{Y_β} = increment in derivative due to modification

σ = side wash angle, deg.

List of Illustrations

1. Introduction

Sub- and supersonic wind tunnel tests of models of the Avro C-105 aircraft have indicated poor directional static stability characteristics at all speeds and at moderate and large angles of attack. As discussed in section 2 of this note, low or negative directional stability would be in fact expected from general considerations of the C-105 fuselage-wing configuration.

The present investigation is concerned with the effects of various modifications, such as additions of ventral fins, wing fins, etc. on the directional stability of the C-105 configuration. The tests were essentially of an ad hoc and preliminary nature, their purpose being to indicate trends rather than to furnish quantitative data.

2. Effects of Fuselage-Wing Configuration on Directional Stability

From theoretical considerations and review of the available experimental data the following factors appear to affect primarily the directional stability of wing-body configurations:

(i) Wing sweepback. Contributes to loss of directional stability with increasing angle of attack (ref. 1).

(ii) Fuselage nose length. The increase in length of the expanding position of the nose has a destabilizing effect at appreciable angles of attack (ref. 1, 6). This is attributed to the corresponding upward displacement of the fuselage vortices which leaves a larger portion of the tail in the unfavourable sidewash field below the adjacent vortex, as indicated in fig. 1b. Wing vortices, particularly with a high wing, would have a similar effect, fig. 1a.

(iii) Fuselage shape. It has been established experimentally (ref. 1, 6)

that square and rectangular fuselage shapes have a destabilizing effect compared to a circular fuselage, even at low angles of incidence. Also, a "tall" rectangle appears to be worse than a "flat" rectangle. The explanation of these effects might be similar to that suggested in (ii) above.

(iv) Wing location (height). The distribution of the wing-fuselage induced sidewash depends on the location of the wing relative to the fuselage and strongly affects directional stability (ref. 1, 3).

With a high wing, the body-induced angle of attack is such as to produce adverse sidewash above the wing wake, as indicated in fig. 1d and in the top diagram of fig. 2. With a low wing, on the other hand, a favourable sidewash results above the wing wake.

The effects of these sidewash fields can be considered separately in relation to the fuselage afterbody and vertical tail.

Considering a wing-fuselage configuration above, with a high wing, there is little change in stability with angle of attack since the after-body moves into an undisturbed, in general favourable, flow region. With a low wing, on the contrary, the afterbody moves out of the favourable and into the unfavourable sidewash regions and therefore the configuration becomes increasingly unstable.

However, the vertical tail contributions for the above two cases are opposite to the afterbody contributions and tend to override the former. For the high wing arrangement, the tail is located in an adverse sidewash field, fig. 3, and its contribution decreases with angle of attack. With the low wing, the tail is favourably located and its contribution increases with increasing

incidence, but, due to the destabilizing effects on the afterbody, also this configuration becomes less stable with increasing angle of attack.

Thus, although in both cases stability deteriorates with lift, the effectiveness of vertical tail is appreciably larger for the low-wing configuration, as indicated by results reproduced in fig. 2.

The combined effects of wing location and fuselage shape are indicated in fig. 4. It is seen that high wing has a particularly detrimental effect when used with a circular fuselage and that a rectangular fuselage decreases the directional stability for all wing locations.

(v) Anhedral (ref. 3). With mid or high wing, anhedral would tend to produce a favourable sidewash above the wing similar to that for a low-wing configuration, fig. 1 c.

(vi) Mach number. In general, the directional stability deteriorates with increasing Mach number, due to decrease of lift-curve slope of the vertical tail (ref. 3).

When examined, even superficially, against the above background, the C-105 configuration, characterized by a high wing and a substantially rectangular, long-nose fuselage, would be expected to have unfavourable directional stability characteristics. This has been confirmed by wind tunnel tests carried out to date, their results being shown in fig. 6. The value of the directional stability parameter C_{n_β} is very small at low speeds ($M \approx 0$), and becomes negative at moderate angles of attack (between 5 to 10 deg.) at supersonic speeds.

Although it has been proposed to equip C-105 with an entirely automatic "artificial stability" system, it would be undoubtedly desirable to achieve directional stability by aerodynamic means alone. The review of the factors contributing to instability would indicate that, in general, the effectiveness of aerodynamic surfaces would be greater if they were located below the wing rather than above it, and away from the plane of symmetry. The former point is demonstrated by the results reproduced in fig. 5, which shows a ventral fin to be superior to a dorsal one. Also, a chordwise extension of the main fin, which is located in the wake of the wing, appears to be less effective than a tip extension. The results of a series of tests of various modifications, based on the above considerations and intended to improve the directional stability of the C-105 configuration, are reported below.

3. Description of Tested Modifications

The 1:80 scale model of the C-105 was the one described in ref. 9. The standard C-105 configuration and 5 different modifications were tested. Dimensional details of the modifications are given in fig. 7 and 8 and photographs of the complete model with three different modifications are shown in fig. 9. The tested configurations are listed in Table 1, in which the projected area ΔS (on the plane of symmetry) of the added surfaces and its ratio to the standard vertical tail area ~~S fin~~ S_{fin} are given.

Modification a consisted of addition of a large central ventral fin of about half the area of the standard fin. In practice the added ventral fin would have to be retractable at take off and landing.

In modification b two small triangular vertical fins were attached to the fuselage at angles of ± 30° to the plane of symmetry and were designed to be within the ground clearance for landing. This configuration was also tested in the NAE low speed wind tunnel (ref.10).

Modification c involved addition of triangular fins to bottom and top wing surfaces, their spanwise location coinciding with the elevator-aileron junction, fig. 8. The total area of the wing fins was equal to the standard fin area. The wing fins were designed to allow ground clearance for landing but would not permit any degree of roll.

In modification d the standard fin was replaced by one of almost double the area, fig. 7, the additional area being provided mostly by vertical and chordwise extension near the tip.

Modification e consisted of addition of two wing fences, located on the wing upper surfaces and having a total area of about half of the standard fin area.

The fins and fences involved in the modifications were made of stainless steel sheet with edges rounded by hand. The enlarged fin, modification d, was fitted with a base and bolted to the fuselage; all other surfaces were soldered to the model.

Modification	Configuration	ΔS, in^2	100 $\Delta S / S_{fin}$
-	Standard	0	0
a	Standard + 1 ventral fin	1.75	49
b	Standard + 2 ventral fins	1.35	37.8
c	Standard + 2 wing fins	3.6	100.8
d	Standard fin replaced by larger fin	7.075-3.573 = 3.502	98
e	Standard + 2 wing fences	1.96	54.8

Table 1. Test Configurations

4. Flow Visualization Tests

It was desired to investigate the flow field around the standard fin in order to determine some of the reasons of its ineffectiveness.

Two brief series of tests were made, at M = 1.57.

In the first one schlieren photographs were taken with standard model at 3.5° angle of attack and zero yaw and at zero angle of attack and 3.5°yaw, in an attempt to find the location of fuselage and wing vortices in relation to the fin. However, no disturbances could be discerned.

The second series of tests was concerned with flow visualization on the upper surface of the wing. The wing surface was sprayed with one coat of

Krylon primer, one coat of Krylon white paint and one coat of varnish, providing a clear white background. Before each tunnel run a mixture of lampblack and kerosene was applied to the surface with a brush. Tunnel runs of 2 to 4 seconds duration were made. The streamline patterns thus obtained were photographed. The tests were carried out at M = 1.57 over a range of angles of attack from 0° to 8° and angles of yaw from 0° to -8°. The tests were made with intakes open and with intakes blocked and faired , with the standard fin in place.

Sketches of typical flow patterns were made from the photographs and are shown in fig. 10. Blocking and fairing of the intakes appears to have little, if any, effect. The flow direction near the base of the fin, at moderate angle of attack and at appreciable yaw, is such as to cause a destabilizing yawing moment. This is similar to the results shown in fig. 2 and 3. It is also interesting to note the marked asymmetry of flow over the windward and leeward wing surfaces. The observed flow pattern, which could result from vortices such as indicated in fig. 1, a and b, would make surfaces mounted on the upper surface of the windward wing ineffective from the point of view of directional stability.

Results reported in ref. 7 and here reproduced in fig. 11 confirm this observation. Low speed measurements of side force on fins mounted on the top surface of a 70° swept delta wing indicated a very marked decrease in the contribution of the windward fin with increasing angle of attack.

5. Force tests

All force tests were made at M = 1.57, Re = 1.61 x 10^6 (based on the mean aerodynamic chord), α_n from -4° to 12° in 4° steps and β_n from -4° to 8° in 2° steps.

In addition to configurations listed in Table 1, modifications a, b, c, e and standard configuration were tested with the standard vertical tail removed.

The three lateral components n, l and Y were measured with respect to the

balance axis, but all coefficients are given with respect to the model axes of which the X-axis was parallel to the fuselage datum line and with the origin located at the centre of gravity (at 28% $\bar{c}$ lengthwise and 6.75% $\bar{c}$ above the fuselage datum line).

The uncertainties in the experimental data were estimated for modification b with the standard fin on at a typical test condition and the results are given below.

Quantity	Uncertainty
$C_n = 0.0028$	$\pm$ 0.00057
$C_l = -0.00451$	$\pm$ 0.00014
$C_Y = -0.0324$	$\pm$ 0.0010
$\alpha = 4.02°$	$\pm$ 0.02°
$\beta = 4.34°$	$\pm$ 0.05°
$M = 1.57$	$\pm$ 0.005

Coefficients C_n, C_l, C_Y are plotted versus β in fig. 12, 13, 14. It is noticeable that their variation is substantially linear in all cases excepting the C_n for configurations containing the standard or enlarged vertical fin.

It is noted from fig. 13 and 14 that zero rolling moment ~~or~~ and zero side force occurred at approximately one degree yaw for all cases. This would indicate some form of asymmetry of the model. The yawing moment curves do not show the same systematic zero shift.

The effects of all, except e, modifications are compared in fig. 16, 18 and 19, with the characteristics of the standard configuration. As indicated in fig. 15, in each case curves are drawn for standard and modified configuration, with the standard fin on and off. The data for modification e have been omitted from this

comparison since this modification showed a marked destabilizing effect and was therefore considered of no interest.

The C_n comparison is given in fig. 16. In view of the non-linearity of $C_n - \beta$ curves for standard (or enlarged) fin-on configurations, C_n rather than C_{n_β} data are given. Because of the difficulty in determination of C_{n_β} for complete configurations, the effectiveness of modifications a, b and c, which do not involve changes in the standard fin, can be judged from fig. 17, in which increase ΔC_{n_β} due to modifications alone and obtained from linear data with standard fin-off is plotted against α_n. Modifications a and b, involving ventral fins, are about equally effective at small and moderate angles of incidence, but modification b has also a stabilizing effect at large α_n, whereas modification a is detrimental in this region. Modification c (2 wing fins) has a powerful effect at all α_n, which appears to decrease rather uniformly with α_n increasing.

Looking now at the $C_n - \beta$ characteristics of the complete configurations, fig. 16, at zero angle of attack the ventral fins (modification a and b) appear to remove non-linearity and appreciably increase stability at small β of the standard configuration. Wing-fins (c) and enlarged fin (d) have no such effects on the linearity of $C_n - \beta$.

At large angles of attack the ventral fins do not produce a marked improvement, whereas the wing fins and the enlarged fin appear to be beneficial.

The effects of the modifications on C_{l_β} and C_{Y_β} are shown in fig. 18 and 19 over the range of incidence tested. The influence of one central ventral fin (a) and of 2 wing fins (b) on C_{l_β} is negligible, the enlarged fin (d) having the largest effect. C_{Y_β}, fig. 19, is appreciably affected by all modifications except a.

6. Comparison with NACA Results

In fig. 20 a comparison of lateral coefficients is made with unpublished NACA data obtained at M = 1.6 for standard configuration with intakes open. There is good agreement for the $C_n - \beta$ curves. At higher angles of attack the values of C_{l_β} and C_{Y_β} are respectively lower and higher than the present test results. The estimated errors for the NACA measurements (ref. 11) are compared with the present ones in the table below.

Quantity	Uncertainty	
	NACA	NAE
C_n	$\pm$ 0.0005	$\pm$ 0.00057
C_l	$\pm$ 0.0002	$\pm$ 0.00014
C_Y	$\pm$ 0.0057	$\pm$ 0.0010
α	$\pm$ 0.2°	$\pm$ 0.02°
β	$\pm$ 0.2°	$\pm$ 0.05°

7. Conclusions

(i) Wind tunnel tests at M = 1.57 and Re = 1.6×10^6 of five modifications of the standard C-105 configuration indicated noticeable and in general favourable effects on the directional stability.

(ii) The variation of coefficients C_n, C_l, C_Y with angle of yaw was linear in all cases except the C_n for configurations containing the standard or enlarged vertical fin.

(iii) Introduction of ventral fins removed non-linearity in the $C_n - \beta$ curves at zero angle of attack and increased C_{n_β} to about 0.0007 per deg.

(iv) Flow visualization tests have indicated unfavourable sidewash at the vertical tail location and in the quarter-span region on the upper surface

of the windward wing.

(v) Nonlinearity in the $C_n - \beta$ curves was not removed by the addition of wing fins or substitution of an enlarged fin. The former appreciably increased directional stability at large angles of attack.

(vi) The addition of ventral and wing fins had small effect on C_{l_β} derivative. All except one modification affected C_{Y_β} derivative.

(vii) Comparison of results with the NACA unpublished data obtained at M = 1.6 shows satisfactory agreement.

References

1. E. C. Polhamus
J. M. Hallissy, Jr.
Effect of Airplane Configuration on Static Stability at Subsonic and Transonic Speeds.
NACA RM L56A09A, May 1956.

2. E. C. Polhamus
Some Factors affecting the Variation of Pitching Moment with Sideslip of Aircraft Configurations.
NACA RM L55E20b, July 1955.

3. M. L. Spearman
A. Henderson, Jr.
Some Effects of Aircraft Configuration on Static Longitudinal and Directional Stability Characteristics at Supersonic Mach Numbers below 3.
NACA RM L55L15a, February 1956.

4. A. Goodman
D. F. Thomas, Jr.
Effects of Wing Position and Fuselage Size on the Low-Speed Static and Rolling Stability Characteristics of a Delta-Wing Model.
NACA TN 3063, February 1954.

5. C. L. Gillis
R. Chapman, Jr.
Effect of Wing Height and Dihedral on the Lateral Stability Characteristics at Low Lift of a 45° Swept-Wing Airplane Configuration as Obtained from Time-Vector Analysis of Rocket-Propelled-Model Flights at Mach Numbers from 0.7 to 1.3.
NACA RM L56E17, September, 1956.

6. F. S. Malvestuto, Jr.
W. J. Alford, Jr.
Effects of Wing-Body Geometry on the Lateral-Flow Angularities at Subsonic Speeds.
NACA RM L55L26a, February 1956.

7. W. Jacobs
Theoretical and Experimental Investigations of Interference Effects of Delta Wing-Vertical Tail Combinations with Yaw.
FFA Report No. 49, Stockholm, 1953.

8. W. C. Williams
H. M. Drake
J. Fischel
Some Correlations of Flight-Measured and Wind-Tunnel Measured Stability and Control Characteristics of High-Speed Airplanes.
NACA Paper Presented at AGARD Meeting, Brussels, August 1956.

9. J. G. LaBerge
Six-Component Supersonic Wind Tunnel Tests of a 1/80 Scale Model of the C-105 Aircraft.
NAE Lab. Memo, AE-46d, HSAL-M-72, October 1956.

10. R. L. Wardlaw
P. J. Pocock
AVRO CF-105 Preliminary Ventral Fin Tests.
NAE Lab. Memo AE-46j, March 1957.

11. M. L. Spearman
R. B. Robinson
C. Driver
Longitudinal and Lateral Stability, Control Characteristics and Vertical-Tail-Load Measurements for 0.03-scale Model of the AVRO CF-105 Airplane at Mach Number 1.41.
NACA RM SL56H27, August 1956.

JvdB/JVT

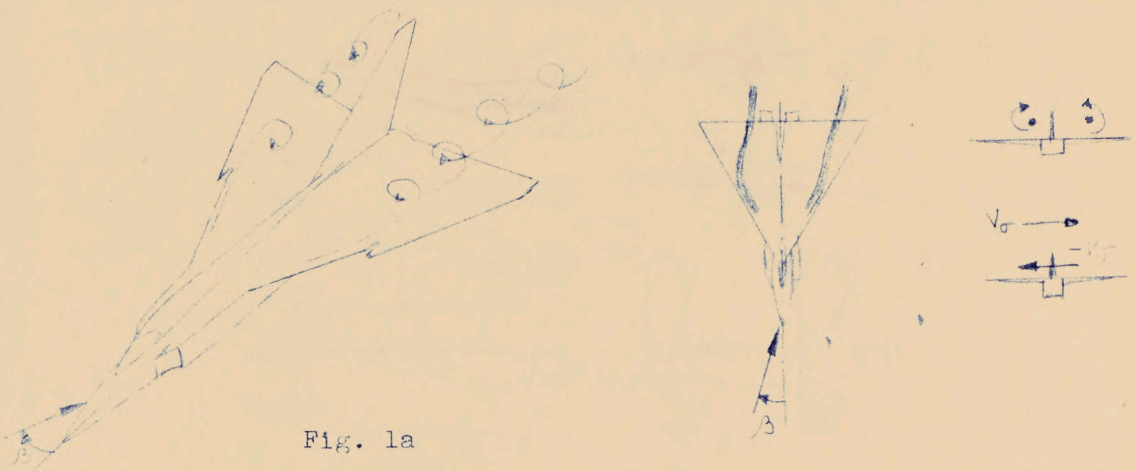

Fig. 1a

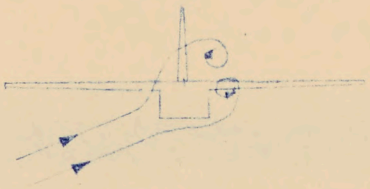

Fig. 1b

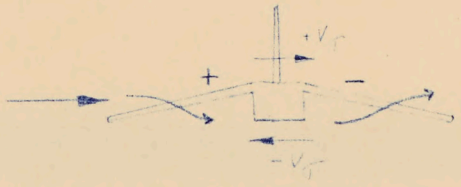

Fig. 1c

Fig. 1d

Fig. 1 Factors influencing sidewash at the fin.

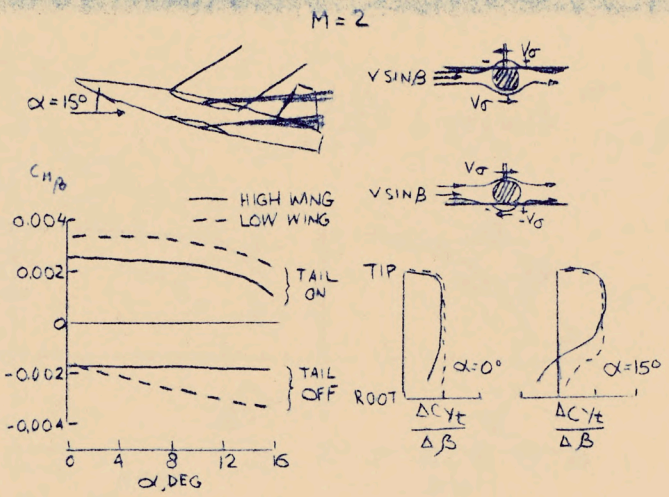

FIG. 8 OF REF. 3

Fig. 2 Effect of wing height on sidewash at the fin

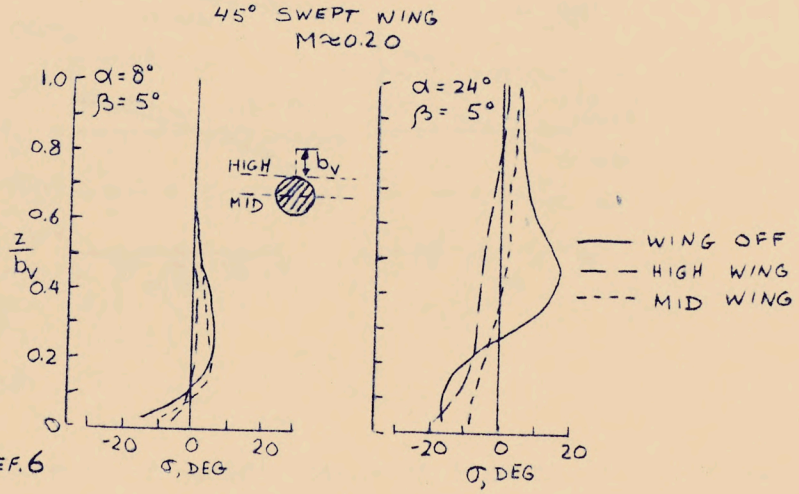

FIG. 6 OF REF. 6

Fig. 3 Sidewash distribution at the fin for two wing heights

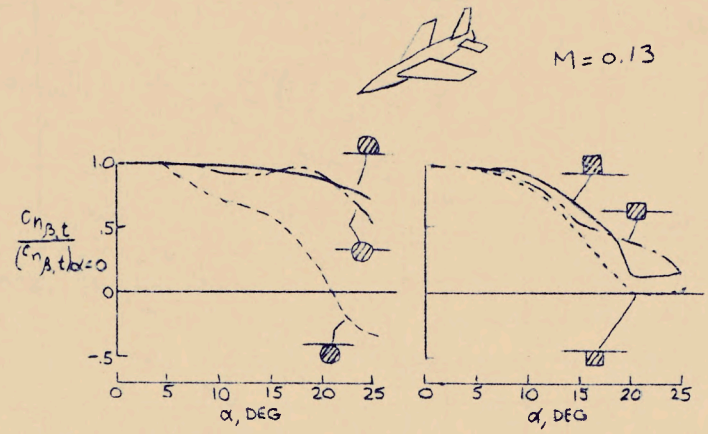

FIG. 7 OF REF. 1

Fig. 4 Effect of wing height on directional stability

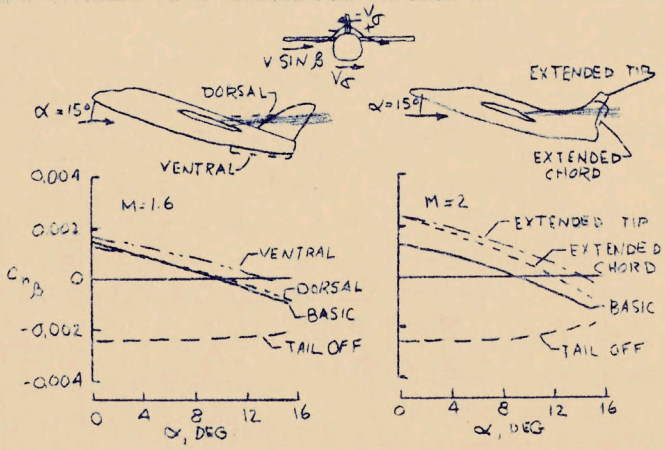

FIG. 9 OF REF. 3

Fig. 5 Effect of modifications on directional stability

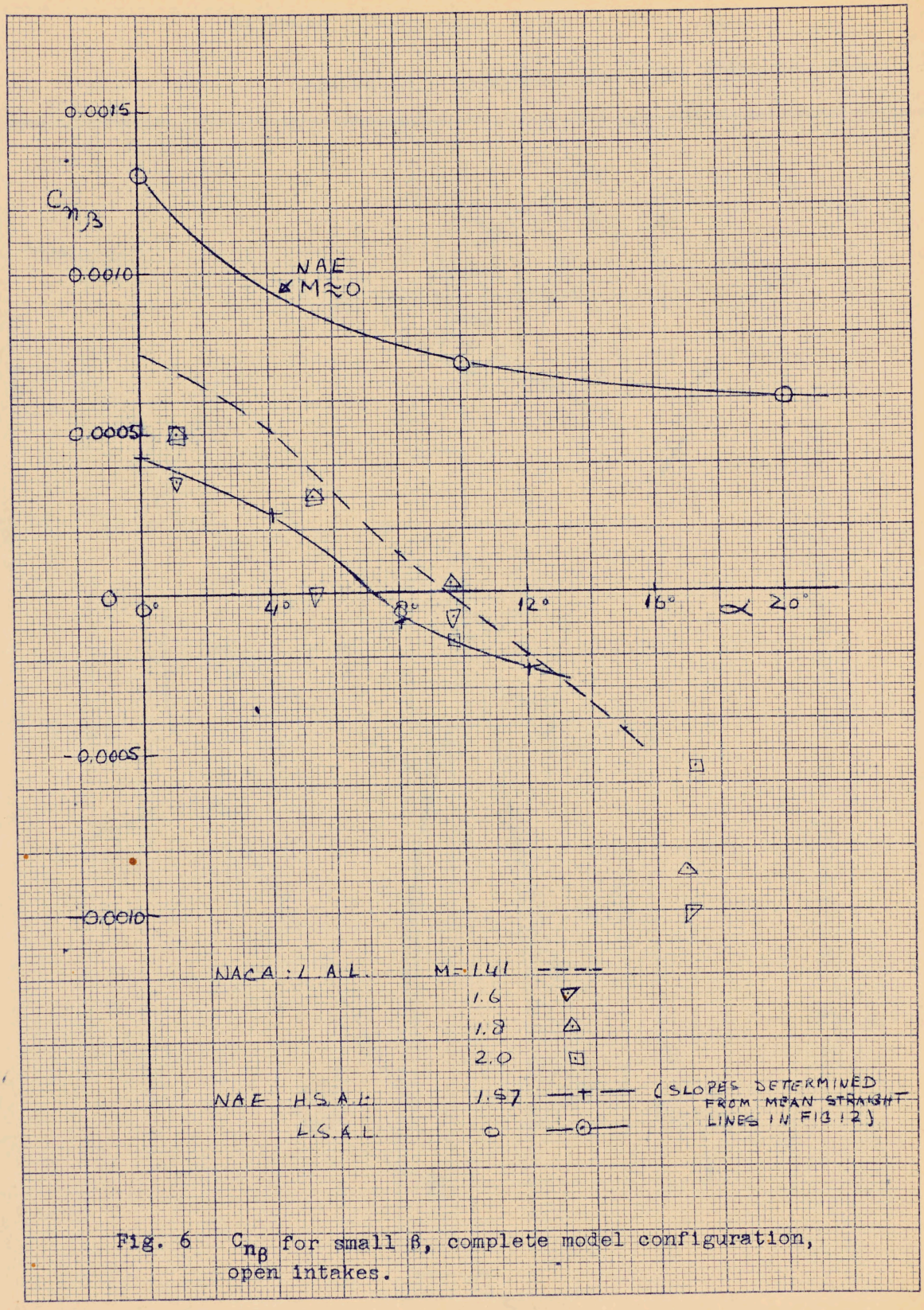

Fig. 6 C_{n_β} for small β, complete model configuration, open intakes.

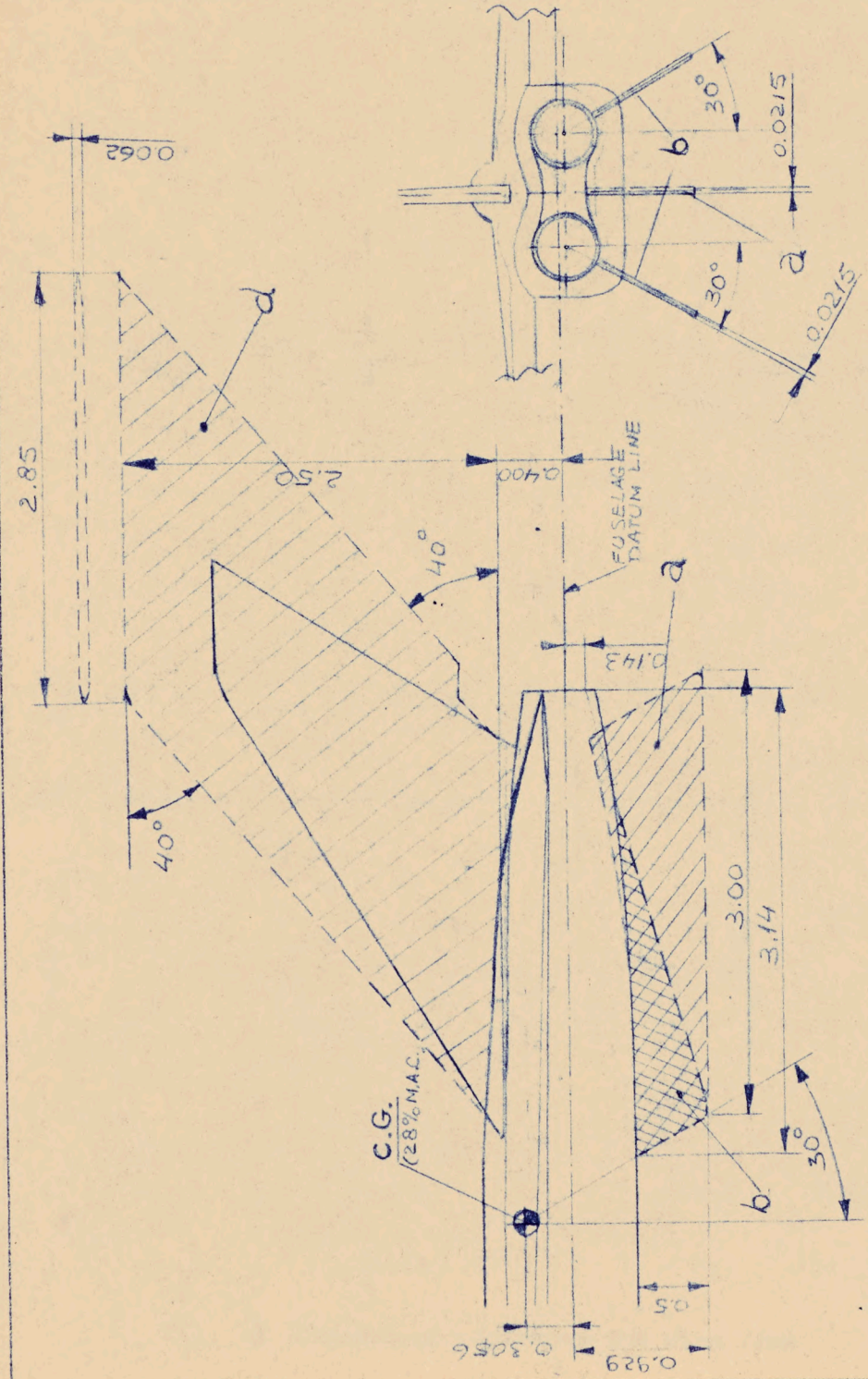

Fig. 7 Dimensions of ventral fins and enlarged main fin

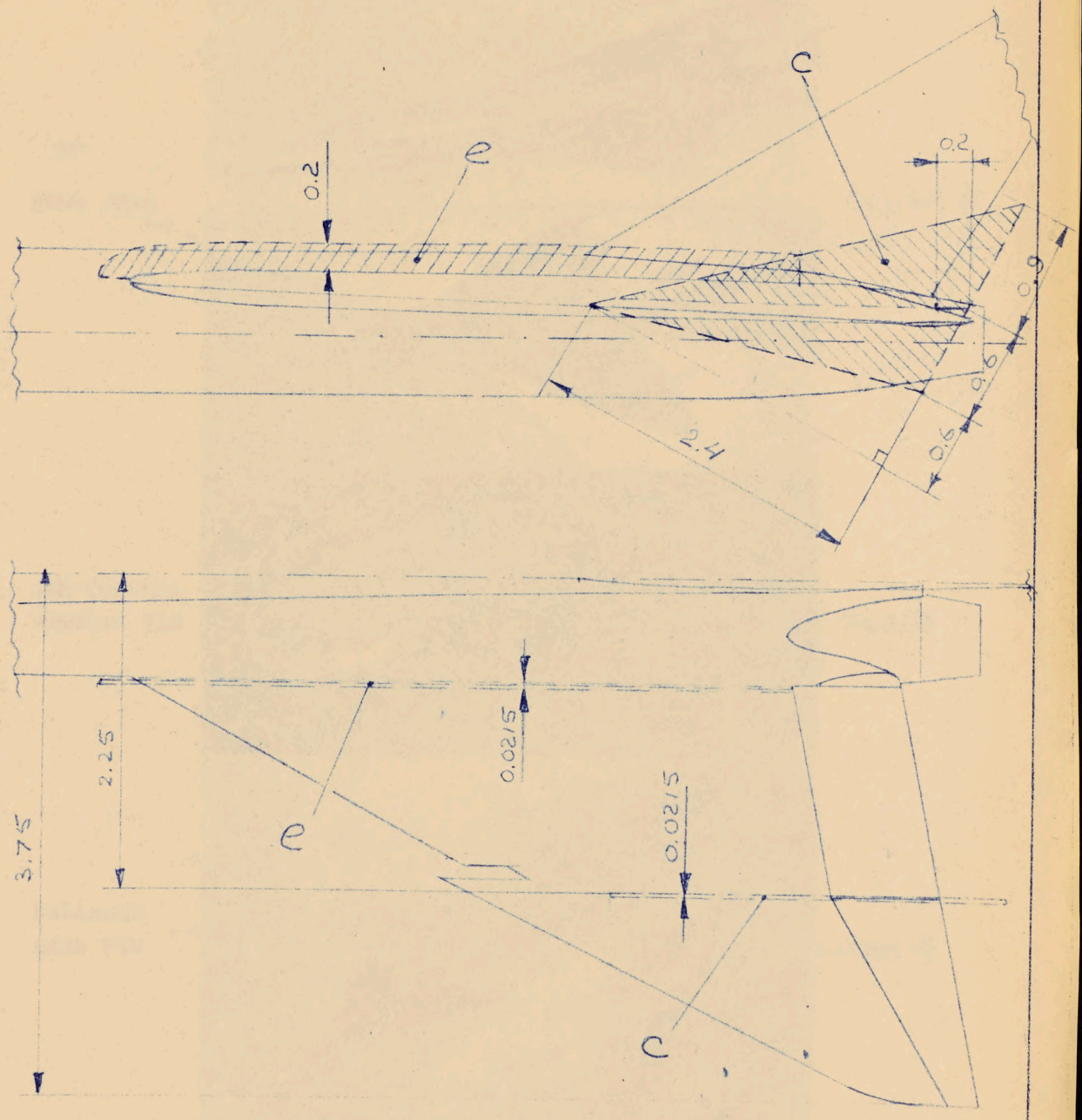

Fig. 18 Dimensions of fences and wing fins

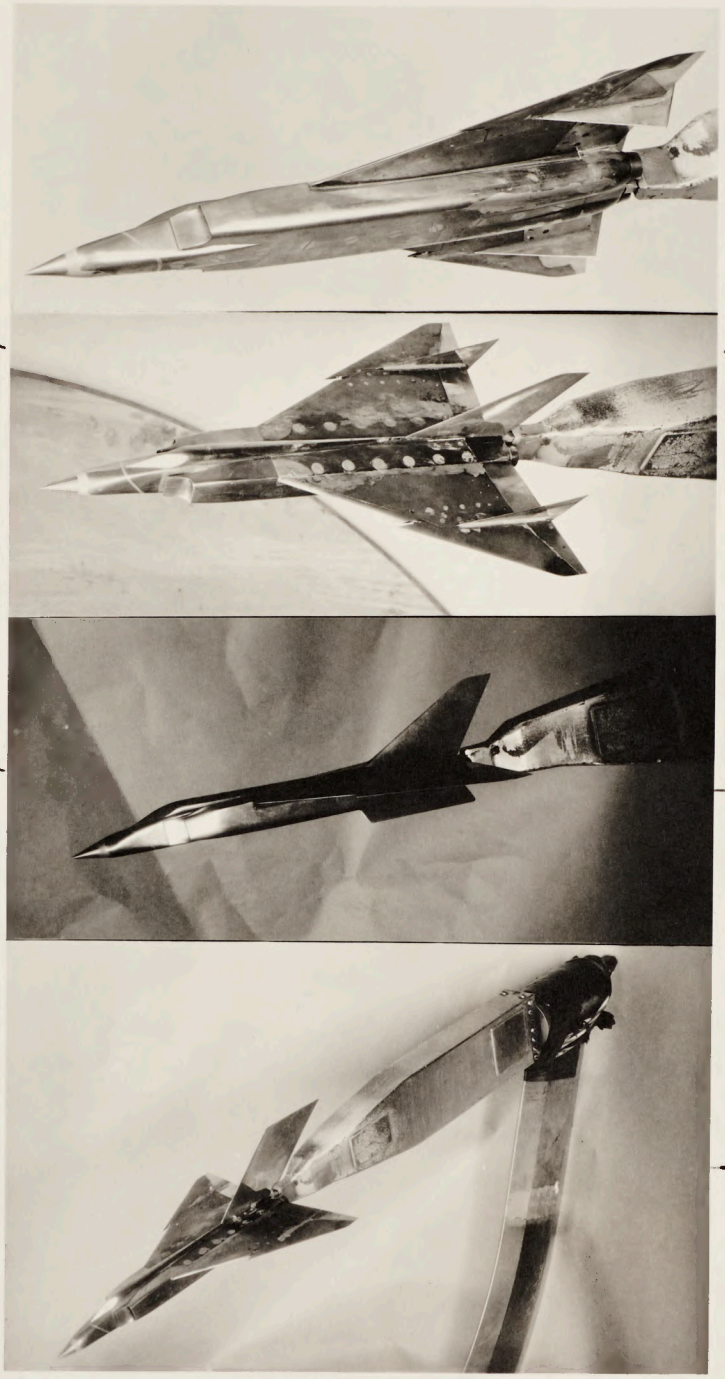

Fig. 9 Photographs of model with some modifications

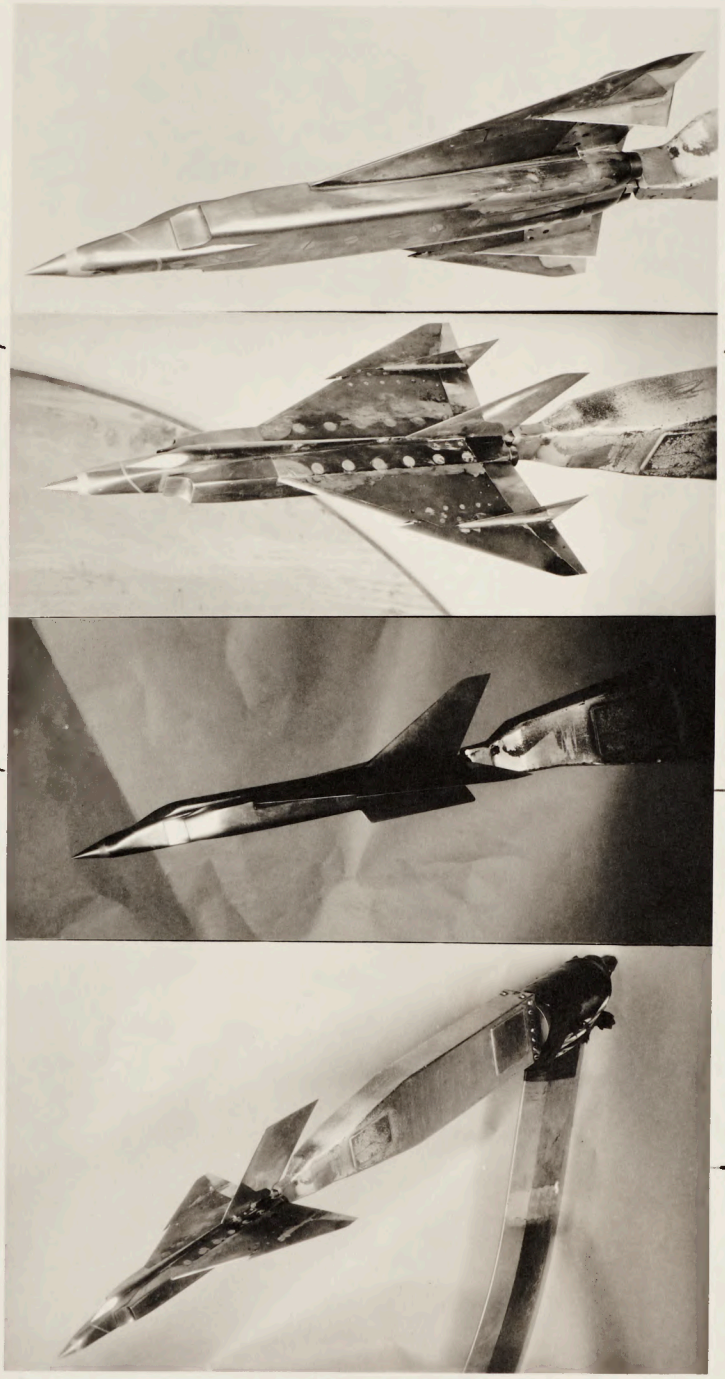

Fig. 9 Photographs of model with some modifications